

A Low-Power Hierarchical FinFET-Based SRAM

Somayeh Maabi¹ Sina Sayyah Ensan² Mohammad Hossein Moaiyeri³
Shaahin Hessabi²

¹Faculty of Computer Science and Engineering, Shahid Beheshti University, Tehran, Iran

²Department of Computer Engineering, Sharif University of Technology, Tehran, Iran

³Faculty of Electrical Engineering, Shahid Beheshti University, Tehran, Iran

Abstract

In this paper, a low-power energy-efficient hierarchical SRAM design capable of working in near-threshold region is proposed. The proposed method enhances the noise margin using an extra circuitry, while restricting the hardware redundancy by sharing the additional circuitry between each two SRAM cells in a hierarchical style. The results of simulating the FinFET-based SRAM cells using Synopsys HSPICE at 10nm technology node indicate that the proposed design reduces, on average, the power-delay product, read and write delays by 14.34%, 2.37% and 8.54%, respectively, and significantly improves the static noise margins even in the presence of major process variations.

Keywords: Static Random Access Memory (SRAM), Multiport Memories, Low-Power Design, Static Noise Margin (SNM), FinFET, Nanoelectronics.

1. Introduction

Nowadays, by scaling the technology node, the variability concerns have become very important. This is due to (i) very small geometries where even small variations can cause big changes, (ii) reduced power supply voltage, where V_{DD} level is very close to transistors threshold voltage [1]. Accordingly, the SRAM cell stability depending on transistors strength ratios has become one of the biggest concerns in VLSI design [2]. With the ever-increasing short channel effects, parametric variations and cache capacity, SRAMs have become very sensitive to variability. As a result, a new trade-off between the variability, power consumption and performance parameters has come in VLSI design [2].

Ignoring redundancy, each cell must work under worst-case variations. In the conventional 6T SRAM, strength ratios of devices must be adopted such that cell static noise margin and write margin are both upheld, while they are in

conflict with each other. During the read state, it is desirable to have stronger storage inverters and weaker pass transistors, while during the write state it is desirable to have stronger access transistors and weaker storage inverters. This fine balance of transistor strength ratios can be easily affected by process variations, which will specifically degrade cell stability and read margin in nanoscale technologies [2].

In order to consider variability problems, many design techniques have been proposed to enable low-voltage operation for SRAM cells. A higher supply voltage can be used for SRAM cells such that the SRAM voltage does not decrease with the technology to meet the desirable margins [3]. However, this approach does not provide the demanded low power consumption. Another approach is to use dynamic voltage sources such that SRAM voltage source can dynamically change during different states [4]-[5]. This technique increases the design complexity, while it improves the cell stability and reduces the standby leakage.

Scaling the technology node has also led to a major power consumption challenge. The importance of power consumptions is more prominent in the systems with restricted energy sources. Reducing the supply voltage is considered as one of the most effective ways to decrease the power dissipation. This is achieved by sub-threshold or near threshold circuits design which enhances energy efficiency [6]. In this way, leakage power is also considerably reduced due to less voltage difference between drain and source of a transistor, which suppresses the DIBL effect, and consequently reduces the OFF current [7].

On the other hand, reducing the supply voltage results in higher propagation delay and slower circuits. At the present time, power saving is becoming very crucial in many circuits and applications that do not require very high speed, such as memories, nano-sensors, radio frequency identification and implantable medical devices. These applications may be in hold or stand-by modes most of the time, and need very low energy consumption and long battery lifetimes [8]. In addition, investigations have demonstrated that the minimum energy can be achieved in the sub-threshold region. In other words, appropriate power-delay product (PDP) can be found in the near-threshold region [9]. In the sub-threshold region, the drain current is defined by Eq. 1 [10].

$$I_{sub} = \mu c_{ox} \frac{W}{L} e^{1.8} \phi_T^2 e^{\frac{V_{GS}-V_{th}}{n\phi_T}} \left(1 - e^{\frac{-V_{DS}}{\phi_T}} \right) \quad (1)$$

where, $n = 1 + \frac{C_{dep}}{C_{ox}}$ is the sub-threshold factor and ϕ_T is the thermal voltage.

A specific and important state of a transistor in a nanoscale digital circuit is the OFF state, where $V_{GS}=0V$ and $V_{DS}=V_{DD}$. The drain current in this state, which is denoted as I_{OFF} , is given by Eq. 2. It can be concluded from Eq. 3 that the I_{OFF} leakage current is reduced exponentially by decreasing the supply voltage.

$$I_{OFF} \approx \mu c_{ox} \frac{W}{L} e^{1.8} \phi_T^2 e^{\frac{-V_{th}}{n\phi_T}} \quad (2)$$

On the other hand, reducing the supply voltage to near-threshold region considerably increases the circuit delay. The propagation delay in the sub-threshold region is almost given by Eq. 3, where K is a suitable fitting coefficient.

$$t_d \approx \frac{KCV_{DD}}{\mu c_{ox} \frac{W}{L} e^{1.8} \phi_T^2 e^{(V_{GS}-V_{th})/n\phi_T}} \quad (3)$$

Due to a significant speed reduction, sub-threshold circuits are often unsuitable for high-performance applications. However, they are practical for some applications, which do not require high-frequency operation but demand ultra-low power consumption, such as wireless sensor networks. However, increase in variations in sub-threshold region can degrade circuit stability [17].

SRAMs occupy a considerable part of the area and dissipate a large amount of power in VLSI chips [16]. Therefore, reducing the power consumption in SRAM cells is a vital issue in low-power VLSI design. As SRAM cells

are often in the hold state, decreasing the static power dissipation of SRAM cells considerably contributes in reducing the total power consumption of a chip. Operating of SRAM in the sub-threshold region can dramatically reduce the leakage power, but it degrades the speed and static noise margin (SNM) of the cell, which should be considered in the design methodology [8].

In order to meet the challenges imposed by transistor scaling, different device structures have been explored as alternatives to the conventional bulk MOSFET. However, considering these technologies, FinFET is more appropriate for scaling the MOSFET to near 10nm feature size [11]. FinFETs demonstrate superior gate control on the channel, lower sub-threshold swing, lower short channel effect and higher scalability. However, width quantization is a challenge in FinFETs, which restricts the design possibilities of FinFET-based circuits such as SRAMs that need transistor sizing for correct operation and robustness. This constraint should be carefully considered and compensated in the design procedure [12].

In this paper, a new hierarchical SRAM cell design, denoted as HSRAM, is proposed with improved SNM and static and dynamic power consumption metrics. The number of transistors in every cell is decreased compared to its counterpart presented in [14], by multiplexing the additional transistors between each two cells, which reduces the power and energy consumptions of the proposed design.

The rest of this paper is organized as follows: In the next Section related work is reviewed. The proposed SRAM cells are introduced and described in the Proposed Design Section. The simulation results and comparisons are given in Simulation Result Section, and finally Summary Section concludes the paper.

2. Related Work

Designing low-voltage memories is demanded to reach lower power consumption. The classic 6T (6-transistor) SRAM cell is shown in figure 1. Assume that the X and Y nodes are stored 0 and 1 values, respectively, as illustrated in figure 1. In this case, M1 and M4 are ON and M2 and M3 are OFF. During the hold time, when WL is 0, M5 and M6 are OFF. In this state, the leakage current through M3 can proportionally lead to failure, since in the idle mode the leakage current through M2 and M5 causes a small increment in the voltage of node X, which is not acceptable due to small SNM in sub-threshold region.

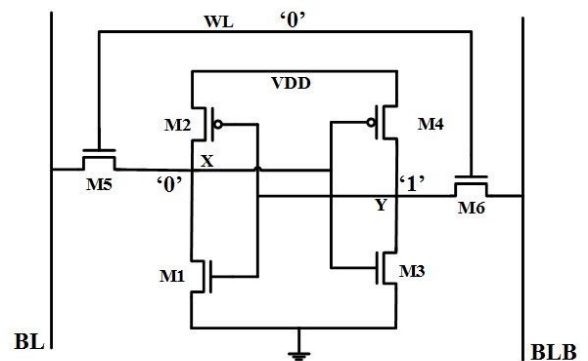


Figure 1. 6T SRAM cell

During the read cycle, when $WL=1$ and $BL=BLB=V_{DD}$, M5 and M6 are ON and consequently, BL will be discharged through M1 and M5, and read operation is accomplished. In this situation, due to existence of some leakage through M3 there is a drop in Y, which results in reading speed degradation and possible data flips on storage nodes. In addition, transistor sizing is not adequate to prevent failures, especially in near- and sub-threshold regions [13].

The 11T SRAM cell [14], illustrated in figure 2, improves the whole energy consumption, the ability of working in sub threshold supply voltages the SNM of the 6T SRAM cell but with the penalty of higher number of transistors and larger area. However, the power consumption specially static power, is the critical challenge in designing digital systems especially in SRAMs.

As the 11T and 13T SRAM cells [14] focus on reducing the static power consumption and improving the performance at sub-threshold region, we discuss these cells in more detail. In the 11T cell, M2, M4, M5 and M6 transistors keep the aforementioned characteristics of the 6T cell. However, the size of the M1 and M3 transistors are scaled down equal to the size of the p MOS transistors. In addition, separate BL, WL and RDWL (read word line) lines are considered in this cell, which leads to separated read and write ports.

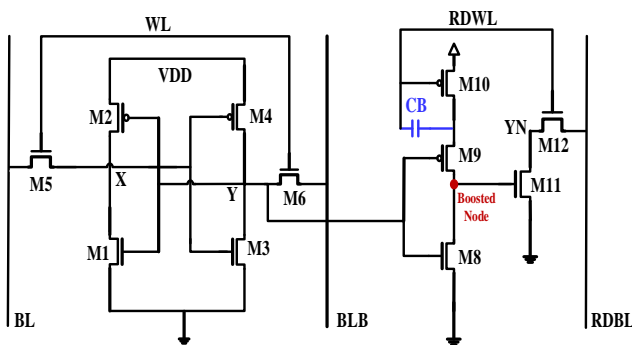


Figure 2. The 11T SRAM cell [12]

During the hold state, the WL and RDWL lines are not activated. Suppose the situation when $Y=0$ and $X=1$, as described before for the 6T cell. In the additional 5T circuitry, M12 is OFF and the state of M11 depends on the voltage at node Y. When $Y=0$, M8 is OFF and M9 is ON, and consequently the gate of M11 is charged. Therefore, a path is created through M11 that connects the node YN to zero. The transistors of the added 5T circuit have minimum size, except the access transistor (M12) that has a larger size.

The boost capacitor (CB) that connects the source of M9 to RDWL is a substantial part in this cell. Given that $Y=0$ (during the hold and write times) and RDWL is connected to ground, CB starts to charge up to V_{DD} . Though, the amount of charging is limited by M9 and finally the maximum voltage reaches $V_{DD}/2$. Thus, the gate of M11 is connected to a voltage of approximately less than $V_{DD}/2$ and YN discharges to the ground slowly.

When RDWL is selected, the source of M9 rises to $1.5 V_{DD}$ and the gate of M11 connects to a voltage higher than V_{DD} . This enhances the read current by an order of magnitude as compared to the classical 6T SRAM cell, which leads to faster read operation. In the other case when $Y=1$, M8 is on and M11 is off, which makes the reading path isolated from the ground. Although the leakage through M11

causes some reduction in the RDBL voltage, this leakage has no effect on YN or RDBL because of connecting M9 to ground via M8.

To suppress the channel leakage path through M8, a modified topology denoted as 13T cell is suggested in [14]. This cell which has 13 transistors is shown in figure 3. When Y is high the source of M8 is connected to ground through the added inverter, but when Y stores “0”, the source of M8 is connected to V_{DD} , which suppresses the leakage path in M8 during the read cycle.

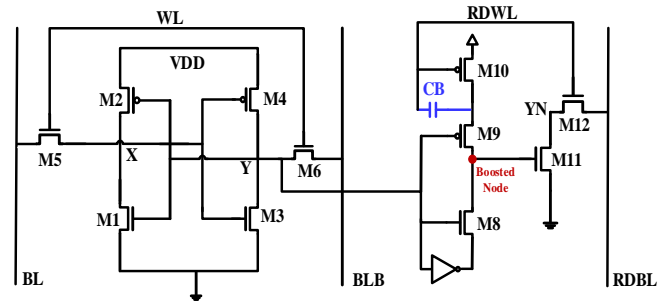


Figure 3. An improved 11T SRAM cell (13T SRAM) [12]

3. Proposed Design

Design of low-voltage digital circuits operating in near- or sub-threshold regions has emerged as a low-power solution for applications with energy constraints. As SRAM memory constitutes a significant percentage of the whole power and area of most digital chips, reducing its power consumption, especially at the stand-by mode, is quite important.

As stated before, the 6T SRAM cell is not suitable for low-voltage applications as it has a small SNM. Accordingly, some effective solutions for improving its SNM in low voltages have been presented in the literature [14]. Despite the improvements in SNM, adding 5 to 7 transistors to the 6T SRAM cell increases the hardware overhead, and consequently the delay and power consumption in the memory system. As a result, for designing an SRAM that maintains the aforementioned SNM improvements, while restricting the hardware redundancy, delay and power, a new hierarchical SRAM (HSRAM) cell is proposed in this paper. The proposed SRAM cell is shown in figure 4. In the proposed design, the hierarchical style also reduces the cell power consumption by use of a multiplexer in the reading path. In this design, due to separating the reading part from the cell, no current is drawn for reading from the cell. Unlike the 6T cell, the read SNM of the proposed cell is not degraded, and is similar to its hold SNM.

As illustrated in figure 4, for reducing the hardware overhead in the 11T SRAM, instead of adding five transistors for each cell, these 5 additional transistors can be shared between each two cells. In this design, the read lines are connected to each other, and the write lines for each cell are separate, as the write ability should be provided for every cell in an SRAM. In order to read from these SRAM cells, a transmission gate-based 2:1 multiplexer is utilized, which connects the SRAM core cells to the read stage. It is worth mentioning that by connecting the read lines, the data stored in each core cell does not become faulty and it is not corrupted during the read procedure.

In the read state, the read line is activated for each of the two cells, and the multiplexer connects the corresponding core cell to the 5-transistor read stage based on the selector signal. If the selector signal becomes '0', the first cell is chosen; otherwise, the second cell is selected. It is noteworthy that the transmission gate structure of the multiplexer provides low-resistive paths and full-swing signals for the read stage.

In addition, the additional inverter existing in the original circuit [14] is omitted in the proposed design as it does not have any considerable effect on the static power, while omitting these two transistors reduces the overall switching power of the SRAM. It is worth pointing out that sharing the read stage also leads to a considerable reduction in the read bit line (RDBL) and read word line (RDWL) capacitances, and consequently results in lower dynamic power consumption and higher speed.

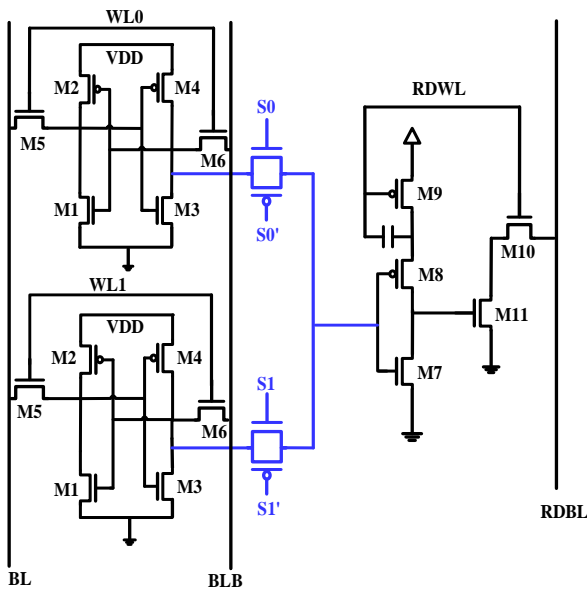


Figure 4. The proposed SRAM (HSRAM)

By categorizing the memory cells and integrating the read line, changing the addressing model of the SRAM cells is necessary. As there is one read line activation for each two cells, according to the conventional models, some clusters of cells may be activated and put on the output simultaneously, which leads to data collision. For solving this problem, the address is divided into two 2-bit parts.

The least significant bit is used as the selectors of the clusters. This bit can be 0 or 1, which will select one of the two cells of each cluster, and the remaining bits will choose the corresponding cluster, and accordingly the corresponding cell is selected to put its data on the output line. These two addressing models are illustrated in figure 5.

4. Simulation Result

The circuits are simulated using the HSPICE simulator tool with 10nm LSTP FinFET technology [15] at 0.45 V supply voltage and at 60°C temperature. Some of the important parameters of the utilized model are given in table 1. In the simulations, all the SRAM's transistors have the minimum size except the ones in the 6T conventional SRAM cell, which have multiple sizes in order to have a good Read SNM. The capacitors of the BL, BLB, RDBL and RDWL lines are assumed as 10fF for a basic design. The power consumption, read and write delays, average case power delay product (PDP), best case PDP, worst case PDP and SNM of the proposed SRAM cell are calculated and compared with those of the other low-power SRAM cells.

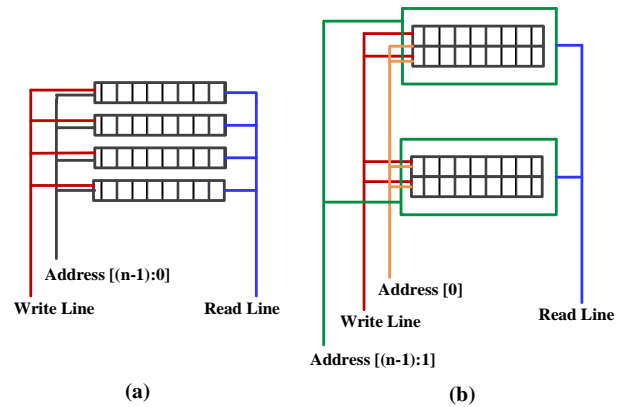


Figure 5. Two addressing models: (a) Conventional model (b) HSRAM Model

Table 1. The FinFET parameters

Parameter	Description	Value
L_g	Physical Gate Length	14 nm
H_{Fin}	Fin Height	21 nm
T_{Fin}	Fin Thickness	8 nm
EOT	Equivalent oxide thickness	0.68 nm
N_{body}	Doping of the body	$2.5 \times 10^{16} \text{ cm}^{-3}$
N_{sd}	Doping of the source-drain regions	$3 \times 10^{20} \text{ cm}^{-3}$
Φ_{gn}	Work Function of the gate for N-type Transistor	4.42 eV
Φ_{gp}	Work Function of the gate for P-type Transistor	4.75 eV

The simulation results for all SRAM cells are given in table 2 Average PDP is the multiplication of average power and average delay. Best case PDP stands for the product of the average power and best delay, while worst case PDP stands for the product of the worst dynamic power and the worst delay. According to the results, the proposed cell has lower power, write delay and PDP than the other designs. This is because of different structure and operation as compared to 6T, and lower number of transistors and less line capacitance in comparison with 11T and 13T cells.

Table 2. The simulation results at $V_{DD}=0.45V$

SRAM	Average Power (nW)	Static Power (pW)	Read Delay (ps)	Write Delay (ps)	Average Case PDP (aj)	Best Case PDP (aj)	Worst Case PDP (aj)
HSRAM	24.81	286.04	311.85	173.11	5.3080	3.8930	19.72
6T	25.60	307.30	319.46	212.64	6.6243	4.7376	20.86
11T	52.91	274.98	244.31	173.86	10.216	8.4497	33.16
13T	36.81	298.11	245.08	177.27	7.1120	5.8346	23.08

Read access delay, which is the time required to discharge RDBL to “ $0.8 \times V_{DD}$ ” after RDWL reaches to $V_{DD}/2$, is one of the metrics in SRAM cells. During read operation, RDWL is activated and the access transistor is turned on. If the data which is going to be read is ‘0’, then RDBL will be discharged to ground; and if the data is ‘1’, no change happens in RDBL. According to the results, the read delay access of the proposed HSRAM is 27.24% and 21.65% longer than those of the 13T and 11T SRAM cells, respectively, due to the multiplexer stage, but 2.37% lower than the 6T SRAM since it has a separate read circuitry. However, the proposed method considerably improves the power consumption and PDP metrics as compared to other cells.

Another important metric in evaluation of SRAM cells is the write access delay, which is defined as the time required to charge the node that has stored 0 to $V_{DD}/2$ after WL reaches to $V_{DD}/2$. During write operation, WL is activated and access transistors are turned on. Then, new data is transferred by these transistors to cell. Write delay access of the proposed HSRAM is 2.4%, 0.43% and 22.8% lower than the 13T, 11T and 6T cells, respectively. In the 6T SRAM, in order to have read ability, the size of transistors are different, and therefore, they do not have the same strength. On the other hand, as the pull down transistors have higher strengths than the access transistors, the write delay gets longer.

The delay, power consumption and PDP of the cells versus supply voltage are plotted in figure 7 and figure 8, respectively. According to the results, the proposed cell has lower power consumption and PDP as compared to the other cells in a wide range of supply voltages, especially at lower voltages.

Static noise margin (SNM) is an important metric in evaluating the robustness of an SRAM cell. The SNM parameter is calculated as the diameter of the biggest square found in the butterfly graph of a SRAM cell. For analyzing SNM, Monte Carlo analysis with Gaussian distribution with 10% variation at the 3-sigma is conducted. Process variations are considered in the Fin height, Fin width and channel length as the important FinFET device parameters. Finally, the diameter is measured in the butterfly graph. The butterfly graphs indicating the hold and read SNMs of the propose SRAM cell are illustrated in figure 7.

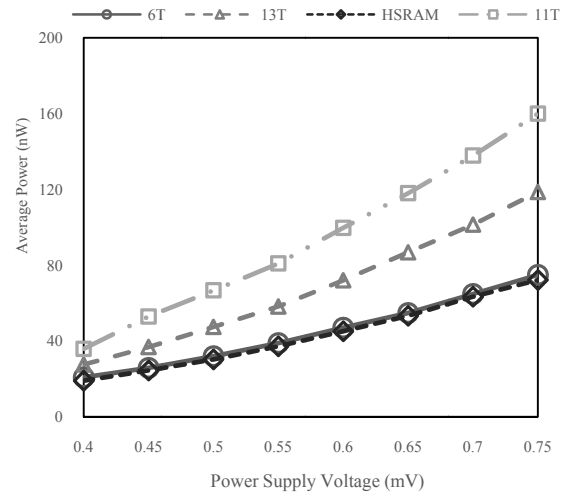


Figure 6. Average Power of the FinFET SRAM cells (T = 60 °C)

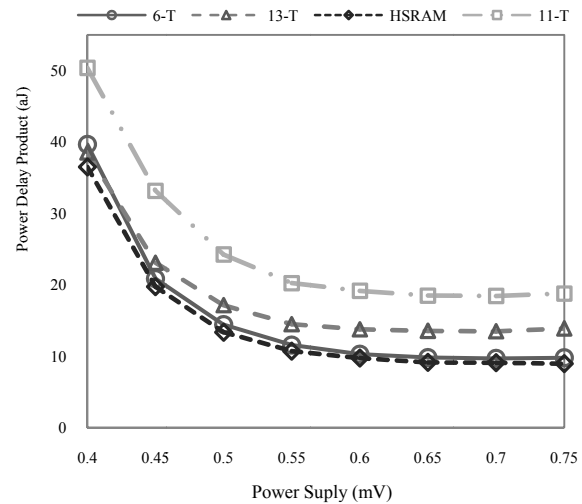
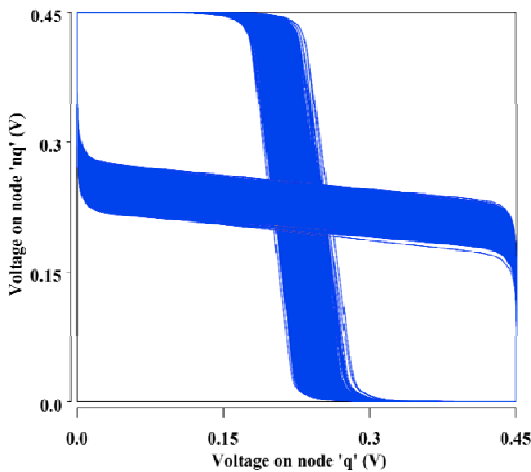
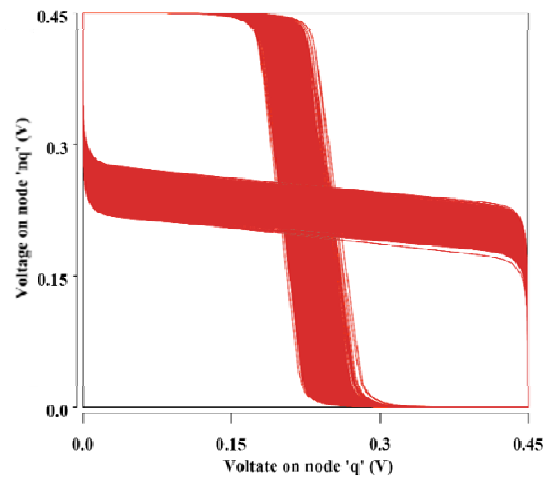


Figure 7. PDP of the FinFET SRAM cells (T = 60 °C)



(a)



(b)

Figure 8. The butterfly curves of the proposed cell (a) Hold (b) Read

Table 3 gives the hold and read SNMs, as well as their variations for the SRAM cells. According to table 3, the hold SNMs for all cells are almost comparable. In the read state, the proposed cell as well as the 11T and 13T cells has SNMs equal to their hold state as there is no charge sharing between the separated read bit line and the main cell. However, in the 6T SRAM cell, due to connecting the cell to BL and BLB, the pulling current (charge sharing) from the cell decreases the read SNM.

Table 3. SNM of the SRAM Cells ($V_{DD}=0.45$ V)

SRAM Cell	SNM (mV)	Variation (mV)
Hold		
HSRAM	183	34
6T SRAM	182	34
11T SRAM	182	35
13T SRAM	182	35
Read		
HSRAM	183	35
6T SRAM	78	41
11T SRAM	182	35
13T SRAM	182	35

5. Conclusion

In this paper, a hierarchical FinFET SRAM cell (HSRAM) has been proposed. In this design, each two 6T SRAM cells share an additional five-transistor circuitry to improve design complexity and power consumption, and achieve higher SNM and execution speed in sub-threshold region. For reading from these SRAM cells, each two cells are connected to the shared read circuitry through a 2:1 multiplexer and finally to the SRAM output. It is worth mentioning that by connecting the read lines, the data stored in every cell does not become faulty, and is not corrupted during the reading procedure. The SRAM cells have been simulated using 10nm LSTP FinFET HSPICE model. It was shown that the proposed structure reduces the number of transistors, line capacitance, power consumption and PDP as compared to its counterpart cells.

References

- [1] A. Shafaei, and M. Pedram, Energy-efficient cache memories using a dual-Vt 4T SRAM cell with read-assist techniques. In *2016 Design, Automation & Test in Europe Conference & Exhibition (DATE)*, pp. 457-462, 2016.
- [2] L. Chang, R. K. Montoye, Y. Nakamura, K. A. Batson, R. J. Eickemeyer, R. H. Dennard, W. Haensch, and D. Jamsek, "An 8T-SRAM for Variability Tolerance and Low-Voltage Operation in High-Performance Caches," *IEEE Journal of Solid-State Circuits*, vol. 43, no. 4, 2008.
- [3] J. Davis, D. Plass, P. Bunce, Y. Chan, A. Pelella, R. Joshi, A. Chen, W. Huott, T. Knips, P. Patel, K. Lo, and E. Fluhr, "A 5.6 GHz 64kb dual-read data cache for the power6tm processor," *IEEE International Solid State Circuits Conference (ISSCC)*, Digest of Technical Papers, 2006.
- [4] A. J. Bhavnagarwala, S. V. Kosonocky, S. P. Kowalczyk, R. V. Joshi, Y. H. Chan, U. Srinivasan, and J. K. Wadhwa, "A transregional CMOS SRAM with single logic VDD and dynamic power rails," *Symposium on VLSI Circuits, Digest of Technical Papers*, 2004.
- [5] K. Zhang, U. Bhattacharya, Z. Chen, F. Hamzaoglu, D. Murray, N. Vallepalli, Y. Wang, B. Zheng, and M. Bohr, "A 3-GHz 70-Mb SRAM in 65-nm CMOS technology with integrated column-based dynamic power supply," *International Solid-State Circuits Conference (ISSCC)*, Digest of Technical Papers, pp. 474-611, 2005.
- [6] Y. Yang, H. Jeong, S. C. Song, J. Wang, G. Yeap, and S. O. Jung, "Single Bit-Line 7T SRAM Cell for Near-Threshold Voltage Operation With Enhanced Performance and Energy in 14 nm FinFET Technology," *IEEE Transactions on Circuits and Systems I: Regular Papers*, vol. 63, no. 7, pp. 1023-1032, 2016.
- [7] K. Roy, S. Mukhopadhyay, and H. Mahmoodi-Meimand, "Leakage current mechanisms and leakage reduction techniques in deep-sub micrometer CMOS circuits," *Proceedings of the IEEE*, vol. 91, no. 2, pp. 305-327, 2003.
- [8] M. Moghaddam, S. Timarchi, M. H. Moaiyeri, and M. Eshghi, "An Ultra-Low-Power 9T SRAM Cell Based on Threshold Voltage Techniques," *Circuits, Systems and Signal Processing*, Springer, vol. 35, no. 5, pp. 1437-1455, 2016.
- [9] M. Alioto "Ultra-Low Power VLSI Circuit Design Demystified and Explained, a Tutorial," *IEEE Trans. Circuits Syst. I, Regular papers*, vol. 59, pp. 3-29, 2012.
- [10] J. Rabaey, *Low Power Design Essentials*, first ed., New York, Springer US, 2009.
- [11] J. P. Colign, *FinFETs and Other Multi-Gate Transistors*, first edition, Springer, New York, 2008.
- [12] S. Kumar Gupta, and K. Roy, *Low Power Robust FinFET-Based SRAM Design in Scaled Technologies, Circuit Design for Reliability*, Springer E-Publishing Inc., New York, pp. 223-253, 2015.
- [13] O. Thomas, M. Reyboz, and M. Belleville, "Sub-1V, Robust and Compact 6T SRAM cell in Double Gate MOS technology," *Proc. IEEE International Symposium on Circuits and Systems (ISCAS)*, pp. 2778 - 2781, 2007.
- [14] F. Moradi, D. T. Wisland, S. Aunet, H. Mahmoodi, and Tuan Vu Cao, "65nm Sub-Threshold 11T-SRAM for Ultra Low Voltage Applications," *IEEE international SoC conference*, pp. 113-118, 2008.
- [15] Predictive Technology Model, [Online]. Available at <http://ptm.asu.edu/>.
- [16] S. M. Salahuddin, and M. Chan, "Eight-FinFET Fully Differential SRAM Cell with Enhanced Read and Write Voltage Margins," *IEEE Transactions on Electron Devices*, vol. 62, no. 6, pp. 2014-2021, 2015.

[17] Y. Yang, J. Park, S. C. Song, J. Wang, G. Yeap, and S. Q. Jung, "Single-Ended 9T SRAM Cell for Near-Threshold Voltage Operation with Enhanced Read Performance in 22-nm FinFET Technology," *IEEE Transactions on Very Large Scale Integration (VLSI) Systems*, vol. 23, no. 11, pp. 2748-2752, 2015.



Somayeh Maabi received the B.S. and M.S. degrees in Computer Engineering from Islamic Azad university of Qazvin branch, in 2008 and 2013, respectively. She is currently a PhD candidate in Computer Engineering in Shahid Beheshti University, Tehran. Her research interests include SoC, NoC, fault tolerance, embedded systems, and processor design specially in end nodes of IoT and WSN

E-mail: s_maabi@sbu.ac.ir

Paper Handling Data:

Submitted: 20.09.2016

Received in revised form: 02.11.2016

Accepted: 12.12.2016

Corresponding author: Dr. Shaahin Hessabi,
Department of Computer Engineering, Sharif University
of Technology, Tehran, Iran.



Sina Sayyah Ensan Received his B.Sc. degree in computer engineering from Shahid Beheshti University, Tehran, Iran, in 2014. He is currently pursuing M.Sc. degree in computer engineering at Sharif University of Technology, Tehran, Iran. His research interests

include Low Power Circuits and VLSI design

E-mail: sayyah@ce.sharif.edu



Mohammad Hossein Moaiyeri received the Ph.D. in Computer Engineering from Shahid Beheshti University, Tehran, Iran in 2012. He is currently an Assistant Professor in the Faculty of Electrical Engineering of Shahid Beheshti University. His research interests mainly

focus on nanoelectronic circuit design, Low-power VLSI design, VLSI implementation of MVL and fuzzy logic, and mixed-signal circuit design.

E-mail: h_moaiyeri@sbu.ac.ir



Shaahin Hessabi received the B.Sc. and M.Sc. degrees in Electrical Engineering from Sharif University of Technology, Tehran, Iran in 1986 and 1990, respectively. He received his Ph.D. degree in Electrical and Computer Engineering from University of Waterloo, Waterloo,

Ontario, Canada in 1995. He joined Sharif University of Technology in 1996, and is currently an associate professor at the Department of Computer Engineering. His current research interests include System-on-Chip and Network-on-Chip, optical interconnects, and VLSI design and test. He has published more than 100 refereed papers in the related areas. Dr. Hessabi has served as the program chair, general chair, and program committee member of various conferences

E-mail: hessabi@sharif.edu